Matrix Biology xxx (2011) xxx–xxx

Contents lists available at ScienceDirect

Matrix Biology

journal homepage: www.elsevier.com/locate/matbio

# Age-dependent regulation of skeletal muscle mitochondria by the thrombospondin-1 receptor CD47

Elfaridah P. Frazier [a], Jeff S. Isenberg [b], Sruti Shiva [c], Lei Zhao [a], Paul Schlesinger [a], Julie Dimitry [a], Mones S. Abu-Asab [d], Maria Tsokos [d], David D. Roberts [d], William A. Frazier [a,*]

[a] Departments of Biochemistry and Molecular Biophysics, Cell Biology and Physiology, Washington University School of Medicine, St. Louis MO 63110, United States
[b] Department of Medicine, Vascular Medicine Institute, University of Pittsburgh School of Medicine, Pittsburgh, PA 15213, United States
[c] Departments of Pharmacology and Chemical Biology, Vascular Medicine Institute, University of Pittsburgh School of Medicine, Pittsburgh, PA 15213, United States
[d] Laboratory of Pathology, Center for Cancer Research, National Cancer Institute, National Institutes of Health, Bethesda, MD 20892, United States

ARTICLE INFO

*Article history:*
Received 4 November 2010
Received in revised form 15 December 2010
Accepted 16 December 2010
Available online xxxx

*Keywords:*
Mitochondrial biogenesis
Skeletal muscles
Mitochondria
CD47 receptor
Fast twitch fibers
Slow-twitch fibers

ABSTRACT

CD47, a receptor for thrombospondin-1, limits two important regulatory axes: nitric oxide-cGMP signaling and cAMP signaling, both of which can promote mitochondrial biogenesis. Electron microscopy revealed increased mitochondrial densities in skeletal muscle from both CD47 null and thrombospondin-1 null mice. We further assessed the mitochondria status of CD47-null vs WT mice. Quantitative RT-PCR of RNA extracted from tissues of 3 month old mice revealed dramatically elevated expression of mRNAs encoding mitochondrial proteins and PGC-1α in both fast and slow-twitch skeletal muscle from CD47-null mice, but modest to no elevation in other tissues. These observations were confirmed by Western blotting of mitochondrial proteins. Relative amounts of electron transport enzymes and ATP/$O_2$ ratios of isolated mitochondria were not different between mitochondria from CD47-null and WT cells. Young CD47-null mice displayed enhanced treadmill endurance relative to WTs and CD47-null gastrocnemius had undergone fiber type switching to a slow-twitch pattern of myoglobin and myosin heavy chain expression. In 12 month old mice, both skeletal muscle mitochondrial volume density and endurance had decreased to wild type levels. Expression of myosin heavy chain isoforms and myoglobin also reverted to a fast twitch pattern in gastrocnemius. Both CD47 and TSP1 null mice are leaner than WTs, use less oxygen and produce less heat than WT mice. CD47-null cells produce substantially less reactive oxygen species than WT cells. These data indicate that loss of signaling from the TSP1–CD47 system promotes accumulation of normally functioning mitochondria in a tissue-specific and age-dependent fashion leading to enhanced physical performance, lower reactive oxygen species production and more efficient metabolism.



## 1. Introduction

Mitochondrial biogenesis is regulated by many factors including developmental cues, energy demand, thermal stress, exercise, fasting and hormonal regulators (Lin et al., 2005; Feige and Auwerx, 2007; Leone et al., 2005; Benton et al., 2008). These diverse signals converge on the transcriptional coactivators peroxisome proliferator-activated receptor γ coactivator-1 α and β (PGC-1 α/β). These two coactivators have distinct but overlapping tissue expression and regulatory properties and are themselves regulated at the level of transcription (Lai et al., 2008; Uldry et al., 2006). PGC-1α acts with PPARs (peroxisome proliferator-activating receptors), ERRs (estrogen-related receptors) and NRF-1 (nuclear respiratory factor-1) to coordinate mitochondrial biogenesis and energy metabolism (Finck and Kelly, 2007). Sirt-1, a member of the family of sirtuin deacetylases, thought to have a causal role in longevity due to caloric restriction, has been reported to act upon PGC-1α, deacetylating it and thus facilitating its interaction with NRF-1 to promote mitochondrial biogenesis (Nemoto et al., 2005; Feige and Auwerx, 2008). Calorie restricted mice (Lopez-Lluch et al., 2006), Sirt-1 over-expressing transgenics (Bordone et al., 2007) and mice treated with resveratrol (Lagouge et al., 2006) or its analogs (Feige et al., 2008) have more mitochondria than control mice. Thus, the notion arises that increasing or maintaining mitochondrial biogenesis opposes metabolic syndrome and benefits cardiovascular function and perhaps longevity (Guarente, 2008).

On a molecular level, cyclic AMP is a major activator, via CREB, of the transcription of PGC1α (Wu et al., 2006) and of genes encoding mitochondrial proteins (Carlezon et al., 2005). It has also been reported that cGMP, synthesized by soluble guanylyl cyclase in response to nitric oxide (NO) stimulation, can activate PGC1α expression (Lira et al.-a,b; Nisoli and Carruba, 2006). Therefore,

* Corresponding author at: Department of Biochemistry and Molecular Biophysics, 8231, Washington University School of Medicine, 660 South Euclid Ave, St. Louis, MO 63110, United States. Tel.: +1 314 362 3348; fax: +1 314 362 7183.
*E-mail address:* frazier@wustl.edu (W.A. Frazier).

0945-053X/$ – see front matter © 2011 Published by Elsevier B.V.
doi:10.1016/j.matbio.2010.12.004

pathways that increase both cGMP and cAMP can potentially stimulate mitochondrial biogenesis.

Recently, we discovered that thrombospondin-1 (TSP1) and its receptor CD47 constitute a previously unknown regulatory system that limits the action of NO in all vascular cell types and several tissues (Isenberg et al. (2006a, 2008f)). TSP1 ligation of CD47 blocks the canonical NO signaling pathway at three points: activation of eNOS is inhibited (Bauer et al.), NO stimulation of soluble guanylyl cyclase is impaired (Miller et al.) and stimulation of protein kinase G by cGMP and its analogs is also blunted (Isenberg et al., 2008g). Furthermore, engaging CD47 with TSP1 or TSP1-mimetic antibodies to CD47 results in a dramatic suppression of cellular cAMP levels (Frazier et al., 1999; Wang et al., 1999; Manna and Frazier, 2003; Yao et al., in press). The physiological relevance of this CD47 suppression of cAMP and cGMP is confirmed by the observation that levels of both cyclic nucleotides are elevated in tissues of CD47 null mice (Isenberg et al., 2009; Yao et al., in press). Thus CD47 blunts signaling emanating from both cGMP and cAMP pathways and therefore could potentially limit mitochondrial biogenesis. Since CD47 is widely, if not ubiquitously expressed in mammalian tissues, such an effect might have a significant impact on mitochondrial numbers in many tissues and organs.

To investigate this issue, we have characterized the mitochondrial status of TSP1 and CD47 knockout mice and report here that young mice lacking either TSP1 or CD47 have a greater mitochondrial volume/mass than WTs and this effect is most prominent in skeletal muscle, resulting in muscle fiber type switching and greater endurance relative to WT mice. As WT mice age, skeletal muscle mitochondrial numbers and performance decrease. By ca. one year of age, both TSP1 null and CD47 null mice have lost their increased muscle mitochondrial load, their endurance advantage over WT mice and their enhanced metabolic efficiency. However, aging CD47 and TSP1 nulls remain leaner than matched WTs. Thus TSP1–CD47 signaling limits mitochondrial biogenesis in young skeletal muscle and CD47 knockout has a substantial, but transient impact on muscle physiology.

## 2. Results

### 2.1. Mitochondrial mRNAs are elevated in skeletal muscle of young cD47 null mice

Both cGMP (stimulated by NO) and cAMP (acting via CREB) have been reported to increase mitochondrial biogenesis. TSP1–CD47 signaling can lower cellular levels of both cyclic nucleotides (Frazier et al., 1999; Isenberg et al., 2006b), and both TSP1- and CD47-null mice have elevated levels of cGMP and cAMP in tissues. While TSP1 can bind many receptors, the modulation of cyclic nucleotide levels by TSP1 is mediated via CD47 (Chung et al., 1999; Isenberg et al., 2008b). Therefore we hypothesized that CD47-null mice might have more mitochondria than matched WTs. Quantitative RT-PCR (Q-PCR) of certain "marker mRNAs" is a sensitive way to rapidly survey tissues for their content of mitochondria (Lagouge et al., 2006; Feige and Auwerx, 2007). Here we surveyed the mRNA levels of cytochrome *b* (encoded by mitochondrial DNA), cytochrome *c*, PGC-1α and NRF-1 (all encoded by nuclear DNA) as indicators of the mitochondrial content and ongoing biogenesis in tissues of 3 month old CD47-null mice. As seen in Fig. 1, levels of the mitochondrial marker mRNAs were not significantly elevated relative to WT in most tissues. However, skeletal muscle (soleus and gastrocnemius) exhibited 3- to 5-fold higher expression of all four markers relative to WT tissues from littermates. CD47 is also well expressed in skeletal muscle of WT mice (determined by Q-PCR, not shown). To verify the Q-PCR results at the protein level, we also performed Western blotting of WT and CD47-null tissue lysates from gastrocnemius and, for comparison, from heart ventricle tissue. As shown in Supplemental Fig. S1, skeletal muscle from CD47-null animals had substantially greater concentrations of cytochrome *c* (a soluble mitochondrial protein) and VDAC1 (a mitochondrial membrane protein) in agreement with the Q-PCR results in Fig. 1. In contrast, WT and CD47-null hearts (ventricle) of 3 month old mice had comparable levels of both mitochondrial proteins (Fig. S1). Based on this data and the fact that skeletal muscle represents the largest depot of mitochondrial mass in the body, we elected to examine in detail the mitochondrial phenotype of skeletal muscle from the CD47-null mice.

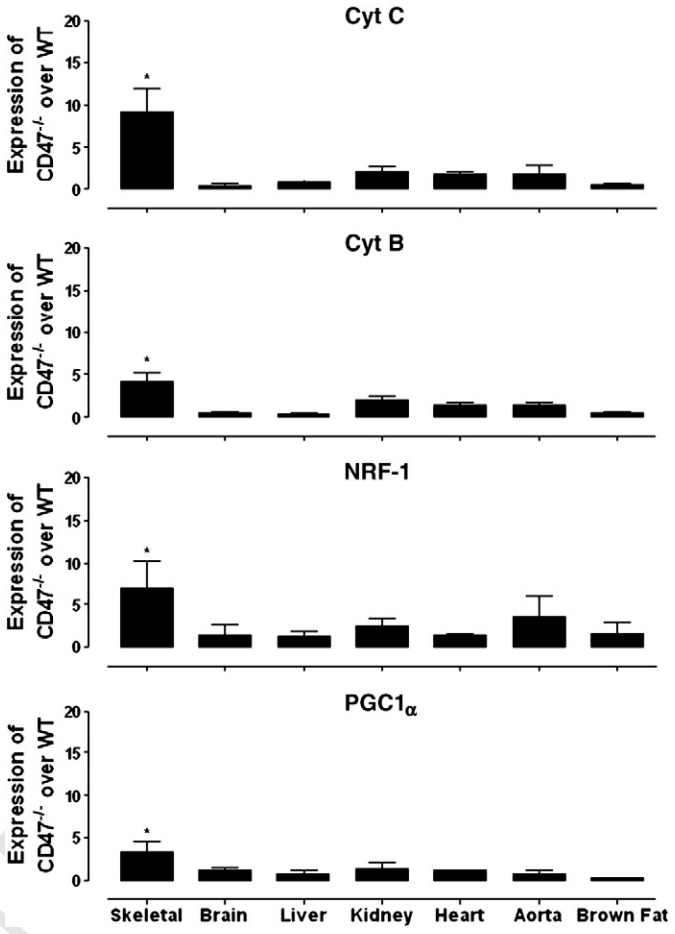


**Fig. 1.** Tissue survey of mitochondrial mRNA expression. RNA was prepared from the indicated tissues with the RNA Later$^{c}$ method and levels of mRNA for cytochrome c (cyt c), cytochrome b (cyt b), nuclear respiratory factor-1 (NRF-1) and PGC1a were determined by Q-PCR using the Sybr Green method. Data is plotted as the ratio of the CD47-null value to the WT value, both of which were first normalized to the level of mRNA for the ribosomal protein 36B4. Tissue from 5 to 16 mice was processed independently for each value shown.

### 2.2. CD47 and TSP1 null skeletal muscle contain more mitochondria than WT muscle

Skeletal muscle from WTs and C47 nulls was examined with thin section transmission electron microscopy. The WT muscles showed the stereotypical pattern of myofibrillar bands with long rows of usually single intermyofibrillar mitochondria aligned between myofibrils (Fig. 2A). In clear contrast, CD47-null soleus (Fig. 2B) contained a higher density of mitochondria than its WT counterpart. Mitochondrial volume density calculations indicate nearly a two-fold increase in the volume of mitochondria in CD47-null soleus: wt soleus 6.8% (±0.6%%, sem) vs CD47-null soleus 11.3% (±1.5%%, sem) ($p<0.05$) mitochondrial area per field (Fig. 2C). In addition, the mitochondria in the CD47-null muscle were of a much broader range of sizes than WTs



Please cite this article as: Frazier, E.P., et al., Age-dependent regulation of skeletal muscle mitochondria by the thrombospondin-1 receptor CD47, Matrix Biology (2011), doi:10.1016/j.matbio.2010.12.004

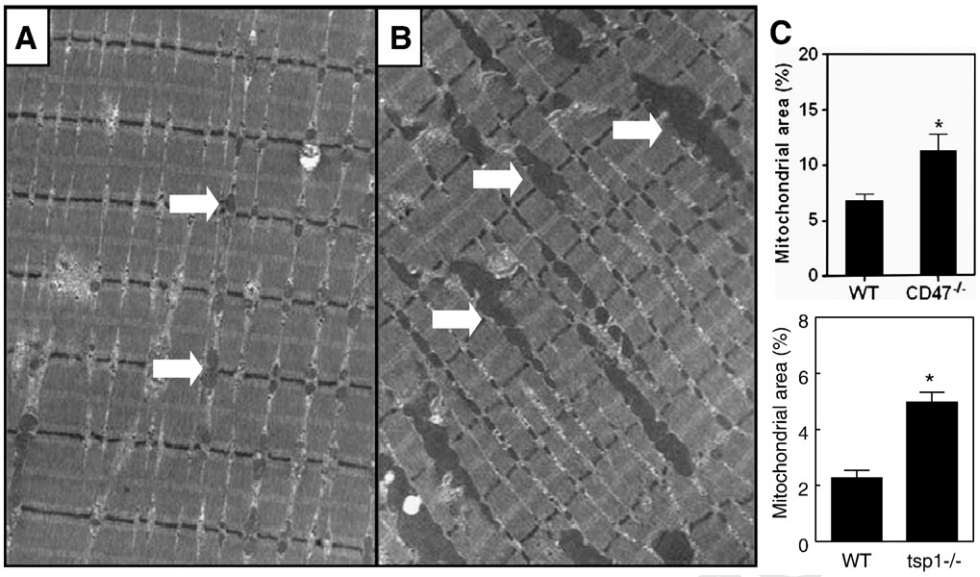


**Fig. 2.** Electron microscopy of soleus muscle from CD47-null and WT mice. Soleus was rapidly harvested and fixed in a mixture of paraformaldehyde and glutaraldehyde and prepared for thin section TEM. WT muscle is shown in A and CD47-null in B. White arrows indicate mitochondria. The final magnification is 10,000× for both. In C, percent mitochondrial area in ten randomly selected fields was measured for each of 3 animals for each genotype. The CD47 null data (top panel) is for soleus, a type I slow-twitch muscle and the TSP1 null data (bottom panel) is for gastrocnemius, a type II fast twitch muscle. Comparable increases were seen in both muscle types in both knockouts.

with many very large mitochondria present (Fig. 2A and B). Clusters of subsarcolemmal mitochondria were observed in both WT and knockout soleus, and these were included in the overall quantification process above. Like the intermyofibrillar mitochondria, the subsarcolemmal mitochondria in CD47-null soleus also had a much wider size variation than those in WT soleus. Similar increases in mitochondrial density and volume were observed in gastrocnemius muscle harvested from 3 month old TSP1 null mice relative to WT (Fig. 2C, Fig. S2). TSP1 null gastrocnemius had 70% more mitochondria, and the mitochondrial volume was two-fold greater than WT (Fig. 2C). As in the CD47 null muscle, there was an increase in the size heterogeneity of mitochondria in the TSP1 nulls (Fig. S2).

In contrast to soleus muscle, electron microscopy of heart papillary muscle from the same mice did not reveal any difference in mitochondrial density (WT 27.2% ±+/−0.1, sem, CD47-nulls 27.4% ±+/−0.8) sem) or appearance between CD47-nulls and WTs. Enzymatic assays of complexes I, II and IV activities (normalized to citrate synthase activity) revealed no significant differences between WT and CD47-null mitochondria from skeletal muscle or liver (Fig. S3). Further, the ATP/$O_2$ ratio of mitochondria isolated from gastrocnemius was not different for CD47-null and WT mice (not shown). Thus, the increased numbers of mitochondria in CD47-null skeletal muscle appear to function normally.

### *2.3. Age-dependent changes in skeletal muscle mitochondria in CD47-null mice*

To determine if the dramatic increase in mitochondria in CD47-null skeletal muscle is maintained as the mice age, we determined the expression of mitochondrial genes (as in Fig. 1) in skeletal muscle obtained from 12 month old CD47-null mice. To our surprise, expression of these genes had decreased to WT levels (which themselves had fallen with age) by 12 months of age (Fig. 3). Mitochondrial content (volume density) in soleus muscle of 12 month old mice was analyzed by quantifying EM images as above. In agreement with the Q-PCR results, the volume density of mitochondria was not significantly different between CD47 null and WT soleus at 12 months of age (CD47-null 6.89 ± 0.30 vs WT 8.86 ± 0.65).

### *2.4. Functional consequences of age-dependent alterations in mitochondrial content*

Endurance training and dietary or genetic manipulations that enhance mitochondrial biogenesis in skeletal muscle often result in increased running endurance (Feige et al., 2008; Lagouge et al., 2006). CD47-null and WT mice (ages 3 and 12 months) were tested in a standard treadmill running protocol. As reported for 3 month old TSP1-null mice (Malek and Olfert, 2009), we found that the young CD47-null mice were able to run nearly twice as long as matched WT controls before becoming exhausted (Fig. 4A). By 12 months of age, the running endurance of WT mice had declined to nearly half that of their younger counterparts, an expected result (Fig. 4A). The running endurance of the 12 month old CD47 nulls also decreased and was no longer significantly different than that of the 12 month old WT mice (Fig. 4A). A similar decrease in endurance was found in the older TSP1 null mice (not shown).

With exercise training, normally fast twitch glycolytic muscle fibers (type II) can switch their phenotype to slow-twitch, mitochondria-rich fibers (type I) (Booth et al., 2002; Holloszy, 2008; Spangenburg and Booth, 2003). Forcing increased mitochondrial biogenesis in skeletal muscle can also convert fast twitch fibers to the

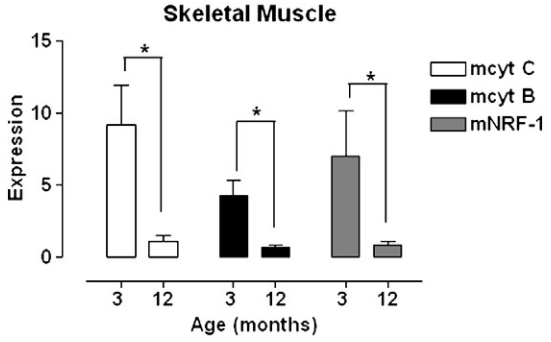


**Fig. 3.** Age-dependent decrease in expression of mitochondrial marker RNAs in CD47 null mice. RNA prepared as in Fig. 1 was amplified using the Sybr Green method. Data is normalized to values for 36B4 mRNA and expressed as the ratio of CD47 null to WT values. At 12 months of age, values for all three RNAs were the same in CD47 null and WT muscle.

Please cite this article as: Frazier, E.P., et al., Age-dependent regulation of skeletal muscle mitochondria by the thrombospondin-1 receptor CD47, Matrix Biology (2011), doi:10.1016/j.matbio.2010.12.004

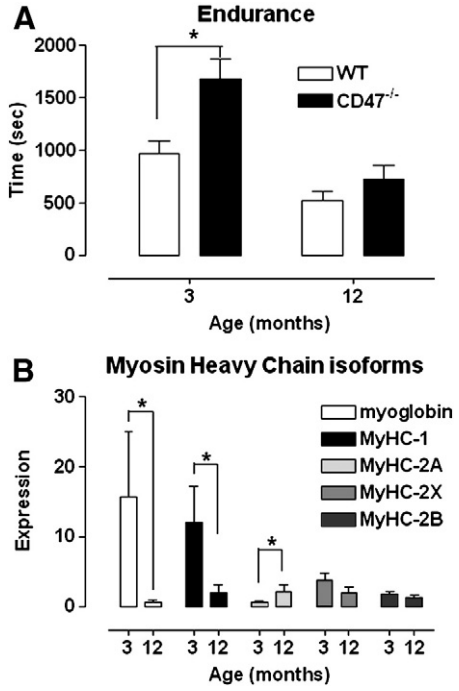


**Fig. 4.** Young CD47-null mice have improved endurance and muscle fiber type switching. (A) Running endurance of 3 month old CD47-nulls is significantly superior to WTs (n = 7–8). (B) CD47-null gastrocnemius muscle, normally a fast twitch muscle, expresses high levels of markers of slow-twitch, mitochondria-rich fibers compared to WT. Q-PCR data expressed as the ratio of CD47-null to WT value for each mRNA as in Fig. 1 (n = 8).

slow-twitch phenotype (Lagouge et al., 2006). As skeletal muscle transitions from fast to slow twitch, expression of myosin heavy chain isoforms shifts from form 2B to 2X, 2A and finally to form 1. As seen in Fig. 4B, gastrocnemius (normally a fast twitch muscle) from 3 month old CD47-nulls had a myosin HC isotype expression profile much more characteristic of slow-twitch fibers with MHC isoform 1 being 23.9 ± ± 12.7 fold over-expressed relative to WT. Myoglobin, another protein enriched in slow-twitch muscle, was 40.9 ± 26.5 fold over-expressed in CD47-null muscle (both MHC-1 and myoglobin expression were significantly greater in CD47-null muscle).

### 2.5. Age-dependent changes in indicators of metabolic efficiency

Accumulation of body fat and increasing weight are hallmarks of aging in mice. At three months of age, CD47-null mice weigh slightly but significantly less than WTs (Fig. 5A). Male and female WTs weighed the same at this age as did male and female CD47 nulls. Identical data was obtained for the 3 month old TSP1 nulls (not shown). The body composition of the CD47 null mice was analyzed with DEXA, revealing that they did in fact have significantly less body fat than WT mice (Fig. 5C). With increasing age, both WT mice and TSP1 and CD47 nulls gained weight, but the weight of both nulls remained significantly lower than WTs over the same interval (Fig. 5A). Thus lack of TSP1 or CD47 limits the age-dependent increase in adipocity normally seen in WT mice.

### 2.6. CD47-null cells generate less ROS than WT cells

Mitochondria are the major cellular source of reactive oxygen species (ROS). We, therefore, determined the ROS production of mitochondria in CD47-null and WT cells using fluorescent indicators of superoxide (dihydroethidium and Mitosox$^{c}$) and other ROS species (dichlorofluorescein). For this study we turned to primary aortic smooth muscle cells (SMC) isolated from male 6 week old CD47-null

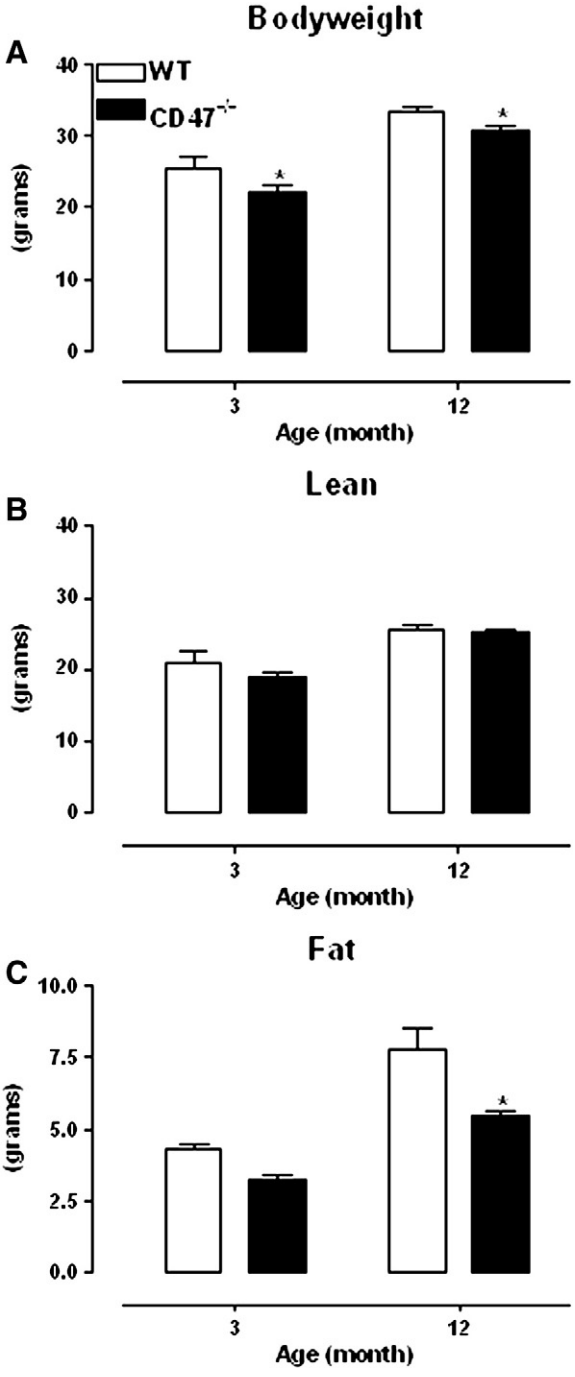


**Fig. 5.** Body composition of CD47 null and WT mice. (A) CD47-null mice weigh significantly less than WTs at both 3 and 12 months of age. Lean (B) and fat (C) body mass were determined by DEXA at both ages. CD47-nulls have significantly less body fat than WTs, accounting for the difference in total body weight (n = 4–6).

and WT mice. The cells were incubated with the indicator compounds and the rate of increase in fluorescence (slope) was normalized to the fluorescence of DAPI as an index of cell number. As detected with Q-PCR and confirmed by Western blotting, the CD47-null aorta, which is composed largely of SMC, also had elevated levels of mitochondrial markers but to a lesser extent than skeletal muscle. However, as seen in Fig. 6, all three reporters indicated a marked reduction in the levels of total cellular superoxide (dihydroethidine), mitochondrial superoxide (Mitosox©) and total ROS (DCF) generation by the CD47-null cells. Therefore, the production of ROS per mitochondrion is very low in the absence of CD47, suggesting that these mitochondria are very efficient. Production of ROS by isolated skeletal muscle mitochondria



Please cite this article as: Frazier, E.P., et al., Age-dependent regulation of skeletal muscle mitochondria by the thrombospondin-1 receptor CD47, Matrix Biology (2011), doi:10.1016/j.matbio.2010.12.004

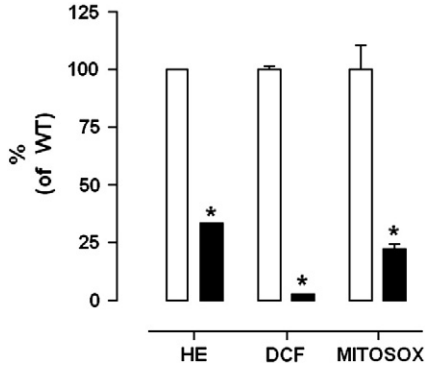


**Fig. 6.** CD47-null aortic smooth muscle cells produce much less ROS that WTs. Early passage aortic smooth muscle cells from male 6 week old null (solid bar) and WT mice (empty bar) were seeded on black 96 well tissue culture plates, grown to confluence, then treated with dihydroethidine which reacts with superoxide to produce fluorescent ethidium (HE), dichlorofluorescein (DCF) which becomes fluorescent after reaction with several types of ROS or Mitosox which detects primarily mitochondrial superoxide. The increase of fluorescence over time (slope) was normalized to cell number determined as the DAPI (nuclear) fluorescence of the same cells. The figure is representative of 3 separate experiments with different batches of cells. Aortic smooth muscle cells were isolated from 6–8 weeks old mice.

in the presence of glutamate (a complex I substrate) was also monitored with the DCF oxidation assay. The rate of DCF oxidation by mitochondria from CD47 null skeletal muscle was not significantly different than that of mitochondria from WT muscle (not shown). Therefore, it is the cellular context in which the mitochondria find themselves that appears to determine their rate of ROS production. In support of this notion, Oxymax respirometry of unstressed 3 month old mice (for a 24 h period) indicated that both CD47 null and TSP1 null mice use less oxygen than WT mice (Fig. S3). Further, production of heat by both knockout mouse strains was lower than that of WT controls (not shown). RER (respiratory exchange ratio), an index of mitochondrial substrate utilization, was significantly elevated in both TSP1 and CD47 null young mice compared to WT littermate controls. Interestingly, all three parameters, oxygen consumption, heat production and RER had returned to WT control levels in the older TSP1 and CD47 null mice. Therefore, mitochondrial density, endurance and cellular and systemic indicators of mitochondrial function all follow the same age-dependent course in TSP1 and CD47 null mice.

### 2.7. Discussion

Mitochondrial biogenesis is regulated in a tissue-specific manner to meet the changing demands of physical activity, dietary energy sources and metabolic and environmental stresses. From aging studies, the concept has arisen that increasing or maintaining mitochondrial numbers and function could be important for extending lifespan or healthspan (Guarente, 2008; Katic et al., 2007; Lopez-Lluch et al., 2006). Many of the signals that affect mitochondrial numbers impinge on the transcriptional coactivator PGC-1α, which acts in concert with NRF-1 to coordinate transcription of the many genes, both nuclear and mitochondrial, that are required to build a functional mitochondrion. PGC1α itself is activated by sirtuin-1 deacetylation, which is thought to promote healthy aging and increased mitochondrial biogenesis (Nemoto et al., 2005; Salminen and Kaarniranta, 2009). We found that skeletal muscle in young (3 month old) CD47 null and TSP1 null mice has a dramatically increased complement of mitochondria. Expression of cytochromes *b* and *c* as well as PGC1α and NRF-1 is significantly elevated in CD47 null skeletal muscle relative to WT levels (Fig. 1). While some other CD47-null tissues sampled (Fig. 1) trended toward higher levels of mitochondrial marker expression than WT, none reached significance. Therefore, the effect of the CD47 knockout to increase mitochondrial numbers appears to be most evident in skeletal muscle. EM analysis of skeletal muscle revealed that the increased numbers of mitochondria appear ultrastructurally normal with the proper electron density and arrangement of cristae (Fig. 2). However, mitochondria in CD47 and TSP1 null muscle exhibit a much wider range of sizes and shapes, perhaps reflecting the role of cAMP-dependent phosphorylation in regulating mitochondrial fission/fusion, i.e., the increased level of cAMP may shift the balance of fission/fusion toward net fusion resulting in larger mitochondria (Chang and Blackstone, 2007; Cribbs and Strack, 2007). Nonetheless, the mitochondria isolated from CD47 null muscle appear to function normally in terms of ATP production and the activity of the electron transport chain enzymes. It is presumably this increased load of functional mitochondria along with the switch to type II fibers that confers a significant endurance benefit on the young CD47 null mice. The similar increase in mitochondria in both the CD47 and TSP1 null mice further reinforces the ligand–receptor relationship of TSP1 and CD47 as seen in numerous studies comparing the phenotypes of these two knockouts (Isenberg et al., 2007a,b, 2008a,c; Maxhimer et al., 2009).

Additional phenotypic alterations in the CD47 null mice may also be related to the early abundance of PGC1α. Interestingly, many phenotypes of the young CD47-null mice closely resemble those of transgenic mice expressing PGC-1α under control of the muscle creatine kinase promoter, which drives expression of PGC-1α in all skeletal muscle at levels 5 to 6 times that in normal fast twitch muscle. This level of PGC1α is similar to the levels seen in type I slow-twitch muscle fibers such as soleus (Lin et al., 2002) (Wenz et al., 2009). In our study, we found a ca. 4-fold increase in PGC1α expression in CD47 null skeletal muscle (Fig. 1). The muscles of the PGC1α transgenic mice that are normally high in type II fibers, e.g. quadriceps, gastrocnemius and others, have more mitochondria and display fiber type switching which contributes to their better endurance just as seen here with the CD47-null mice (Fig. 4). Additional similarities between young CD47-nulls and the PGC1α transgenics (Wenz et al., 2009) include lower weight and less body fat than WTs, lower ROS production, increased sirtuin-1 expression (our unpublished data), increased bone mineral density (Uluckan et al., 2009) and increased muscle vascularization (Isenberg et al., 2007c; Malek and Olfert, 2009).

Since CD47 suppresses both cGMP and cAMP levels and both cyclic nucleotides have been reported to stimulate mitochondrial biogenesis, our hypothesis on beginning this study was that CD47-null mice might have greater numbers of mitochondria in many tissues. However, the dramatic increase in mitochondria limited largely to skeletal muscle in the CD47 knockouts was unexpected. It is interesting that eNOS-null mice have decreased numbers/mass of mitochondria and this deficit is most prominent in skeletal muscle (Le Gouill et al., 2007). Thus the mirror image effects of CD47 and eNOS knockout are consistent with the notion that lack of CD47 increases NO signaling (Isenberg et al., 2008b) which is at least partially responsible for the increase in mitochondria (Lira et al.-a,b). The eNOS-deficient muscles had fewer and smaller mitochondria than WTs, and the mitochondria were somewhat defective in function (Nisoli et al., 2004; Le Gouill et al., 2007). Conversely, mitochondria in the CD47 nulls seem to be more efficient than WTs in terms of their lower production of ROS and the lower oxygen utilization of the mice. As in the case of exercise (Lira et al.-a,b), caloric restriction (Lopez-Lluch et al., 2006), resveratrol treatment (Lagouge et al., 2006), Sirt1 (Bordone et al., 2007) and PGC-1α over-expression (Wenz et al., 2009), the fiber type of fast twitch, type II gastrocnemius muscle in the CD47 nulls showed a pronounced shift to a myoglobin and MHC expression pattern characteristic of slow-twitch, type I, mitochondria-rich muscle. The functional correlate of this switch is seen in the nearly two-fold increase in treadmill time of the CD47-nulls vs WT mice. Therefore, the increase in skeletal muscle mitochondria in the young CD47-nulls and their decrease in the eNOS-nulls may reflect an important and specific role for NO in the regulation of skeletal muscle mitochondria numbers and function.



Please cite this article as: Frazier, E.P., et al., Age-dependent regulation of skeletal muscle mitochondria by the thrombospondin-1 receptor CD47, Matrix Biology (2011), doi:10.1016/j.matbio.2010.12.004

Perhaps the most striking feature of the mitochondrial phenotype of the CD47-null mice is that the differences with WTs seen at three months of age are almost completely gone by one year of age. The decrease in mitochondria density with age occurs in WT animals under normal conditions. Both density and number of mitochondria in quadriceps muscle of WT mice decreased 3-fold between the ages of 2 and 11 months (Corsetti et al., 2008), a time frame comparable to that studied here. In addition the data for WT controls in the PGC1α transgene study evidenced the same age-dependent decline in all functional parameters from 3 to 12 months of age (Wenz et al., 2009). In that study, the continued elevated expression of PGC1α in muscle prevented or slowed much of the age-dependent decrement in mitochondria and muscle performance and other sequellae of aging. In our case, there is a marked decline in mitochondrial transcriptional regulators and the density of mitochondria in the CD47 null mice by one year of age. The functional decline in muscle performance with age is characteristic of sarcopenia, a severe problem for our aging population. It is likely that the effect we observe in the CD47 nulls is due to a more robust biogenesis of mitochondria in young animals that then follows the normal path of decline with age. Consistent with this idea is the elevated expression of PGC1α and NRF1, components that regulate mitochondrial biogenesis, in the young CD47 nulls. The factors that govern the rapid, age-dependent decline in mitochondrial density and muscle function are not yet known. However, it is intriguing to note that expression levels of sirt-1, which deacetylates and activates PGC1α (Rodgers et al., 2005), also drop substantially in skeletal muscle between 3 and 12 months of age (our unpublished data).

In other studies, deletion of either TSP1 or CD47, knockdown of CD47 expression and even blockade of CD47 with antibodies resulted in improved healing of ischemic skin flaps (Isenberg et al., 2007a) and skin grafts (Isenberg et al., 2008e), less damage in ischemia–reperfusion injury models (Isenberg et al., 2008d), reduced stroke damage (Jin et al., 2009) improved vasodilation and cardiac function (Isenberg et al., 2008a) and even protection from ionizing radiation (Isenberg et al., 2008c). A common aspect of many of these models is the generation of ROS. We have seen here that CD47 null cells generate less mitochondrial ROS. Since deletion of either TSP1 or CD47 results in what appears to be a “healthier” or more robust phenotype, we must wonder just what the physiological role of the TSP1–CD47 system might be with regard to mitochondrial homeostasis. It has become clear in recent years that both the content and form of mitochondria are very dynamic, responding rapidly to changes in diet, temperature, hormonal status and likely yet unknown additional factors. The steady state content of mitochondria depends on the balance of biogenesis and removal by autophagy, the preferred mode of disposal and recycling of mitochondria (Scherz-Shouval et al., 2007). Recent literature indicates that autophagy itself is highly regulated and is a necessary process to avoid the accumulation of damaged mitochondria (Scherz-Shouval and Elazar, 2007). This is particularly true in postmitotic tissues such as brain and cardiac muscle. Skeletal muscle is able to regenerate to some extent, calling on a pool of muscle stem cells called satellite cells that exist within muscle fibers, a process that is also sensitive to NO levels (Wozniak and Anderson, 2007). Our finding that the TSP1–CD47 system seems to limit the mitochondrial content of skeletal muscle, at least in young mice, could be due to suppression of mitochondrial biogenesis and/or stimulation of mitochondrial turnover. Further studies will be necessary to determine the mechanism of these effects.

We have shown here for the first time, that lack of CD47 or its ligand, TSP1, causes an increase in mitochondrial density in skeletal muscle, leading to a performance benefit and increased metabolic efficiency. Mitochondria in tissues of the CD47-null mice are more efficient, producing lower levels of ROS, thus reducing the deleterious effects of oxidative damage. The TSP1 and CD47 null mice are also leaner than WTs, suggesting that the enhanced mitochondrial density along with less ROS production may lead to benefits similar to those obtained via caloric restriction and sirtuin-1 or AMP kinase activation. Indeed, the phenotypes of the CD47-null mice are concordant in many respects with those of calorie-restricted mice. Not only does the TSP1–CD47 system limit cardiovascular health (Isenberg et al., 2008f), but it also exacerbates diseases of the aging cardiovascular system (Isenberg et al., 2007b) and may even limit lifespan and/or healthspan. Testing these ideas will require long-term aging studies that may also reveal new aspects of the physiology of the CD47 null and TSP1 null mice.

## 3. Materials and methods

### 3.1. Mice

Wild type and CD47-null C57Bl/6J mice were produced by breeding heterozygotes. The CD47-null line (Lindberg et al., 1996) has been backcrossed to the C57Bl/6J JAX parental strain over 30 times. All mice were genotyped by assessing CD47 expression on red blood cells by flow cytometry and/or by PCR. TSP1 null mice were bed in a pure C57Bl/6J background and periodically backcrossed with WTs to minimize genetic drift. Mice were maintained on *ad lib* chow and water. Genotype was confirmed by PCR. For tissue collection, anesthetized mice were sacrificed by cervical dislocation. Treadmill testing (run to exhaustion) was performed as described (Lagouge et al., 2006). Body fat and lean weight of mice were determined by Dual Energy X-ray Absorptometry (DEXA) in a PIXImus2 scanner according to the manufacturer's protocol (Lunar Corp., Madison, WI). All animal procedures were approved by the NIH or Washington University Committees on Animal Studies.

### 3.2. Real-time quantitative PCR (Q-PCR)

Tissues were harvested and placed directly in RNAlater (Ambion, Applied Biosystems, Foster City, CA) and stored at −80 °C for experiments. A 50–100 mg sample of tissue was homogenized in 1 ml of Trizol (Invitrogen, Carlsbad, CA). Total RNA was isolated according to the manufacturer's protocol, using a high salt solution (0.8 M sodium citrate, 1.2 M NaCl) to yield optimum RNA precipitation. RNA concentrations were determined spectrophotometrically with a Nanodrop spectrophotometer (NanoDrop Technology, Inc., Wilmington, DE). Prior to cDNA synthesis, 1 μg of RNA was treated with 1 μl DNAse I, Amp Grade (Invitrogen, Carlsbad CA) to prevent genomic DNA contamination. cDNA was then synthesized according to the manufacturer's protocol using the iScript cDNA Synthesis Kit (Bio-Rad Laboratories, Hercules, CA) and diluted 1:10. Oligonucleotide primers (Supplemental Table 1) for mitochondrial genes (Duncan et al., 2007), PGC1α, myoglobin and myosin heavy chain isoforms (Oh et al., 2005) were acquired from Intergrated DNA Technologies (Coralville, IA). Constitutively expressed GAPDH and 36B4 ribosomal protein were selected as endogenous controls to correct for any variation in RNA loading. A total reaction mixture of 25 μl consisted of diluted cDNA, 1× iQ Sybr Green Supermix (Bio-Rad, Richmond CA), 200 nM forward and reverse primers. Relative quantification of mRNA was performed using the following thermal protocol: 95 °C for 3 min, 40 cycles at 95 °C for 15 s followed by 55 °C for 40 s for annealing and extension using an ABI 7000 thermal cycler (Applied Biosystems, Foster City, CA). The mRNA expression of gene of interest from CD47-null tissues was expressed relative to the expression of the gene in WTs, which was arbitrarily set to 1.

### 3.3. Western blot analysis

Gastrocnemius and heart ventricles obtained from WT and CD47-null mice and stored in RNAlater at −80 °C were thawed at room temperature and minced. Tissue fragments were transferred to a 0.5 ml centrifugal filter device with a 0.45 μm filter (Amicon,



Please cite this article as: Frazier, E.P., et al., Age-dependent regulation of skeletal muscle mitochondria by the thrombospondin-1 receptor CD47, Matrix Biology (2011), doi:10.1016/j.matbio.2010.12.004

Millipore, Bedford, MA). RNAlater crystals embedded in the tissue were extracted 4–5 times with 80% acetonitrile (Sigma, St. Louis, MO) which was removed by centrifugation at 14,000 rpm for 30 s. Pellets were then collected and protein was extracted using RIPA buffer plus a protease inhibitor cocktail (Roche Diagnostics, Indianapolis, IN) at 37 °C for 1 h. A 20 μg protein sample from each tissue was run on a 4–20% gradient Tris–HCl precast gel (Biorad). Primary antibodies were against cytochrome c (Santa Cruz Biotechnology, Santa Cruz, CA) and VDAC (Novus Biological, Littleton, CO); identical protein loading was determined by pre-staining with Coomassie blue.

### 3.4. Determination of reactive oxygen species

Primary cultures of aortic smooth muscle cells were established as described (Isenberg et al., 2005). Cells from WT and CD47-null mice were matched for sex, age of mice and number of passages in culture (less than 4). Cells cultured in black 96 well plates were shifted to 2% serum for 48 h, and then incubated with DCF (2 ,7 -dichlorofluorescein, Sigma, St. Louis MO), dihydroethidine, or MitoSox (Invitrogen, Carlsbad, CA) in HEPES buffered saline, pH 7.2 at 37 °C in a BioTek (Winooski, VT) fluorescence plate reader in the kinetic mode with readings every 10 min for 2 to 4 h. Cells were fixed in 1% formalin for 15 min and stained with DAPI (Invitrogen) to determine cell numbers with the plate reader.

### 3.5. Electron microscopy

Tissue for electron microscopy was harvested rapidly and placed in a glutaradehyde/paraformaldehyde fixative. Embedding sectioning and staining were carried out as described (Schmidt et al., 2009; Timmers et al., 2008). Ultrathin sections (90 nm) were made and double stained with uranyl acetate and lead citrate, and viewed in a Philips CM10 transmission instrument. Images for analysis were taken at a magnification of 10,000×. The microscopist, (blinded to sample genotype) randomly selected 10 fields (CD47 nulls) or 30 fields (TSP1 nulls) per grid to photograph. Tissues from three different mice were analyzed with at least three sections obtained from each mouse. Mitochondria number and volume density were analyzed using Image J or Image-Pro Plus version 6.2.

### 3.6. Characterization of mitochondria ex vivo

Mitochondria isolated from skeletal leg muscles were assayed for activity of electron transport enzymes as described (Shiva et al., 2007). Determination of the rate of oxygen utilization by isolated mitochondria was performed using a Clark electrode. Isolated mitochondria were also tested for the production of ROS by oxidation of DCF with glutamate as substrate in the fluorescence plate reader in the kinetic mode.

### 3.7. Statistical analyses

All statistical analyses were performed using Prism (GraphPad Software, San Diego, CA). All data are expressed as mean ± SEM of n experiments. The primary comparison was made between matched littermate WT and CD47-null mice. Statistical significance between WT and CD47-null values were assessed with the unpaired t-test, a $P<0.05$ was considered statistically significant.

Supplementary materials related to this article can be found online at doi:10.1016/j.matbio.2010.12.004.

## Acknowledgements

We thank Dr. Robert Schmidt, Director of the Electron Microscopy Core (Washington University School of Medicine) for helpful advice. Drs. Daniel Kelly, Jennifer Duncan, John Lehman, Pamela Manning and John Holloszy, all of Washington University School of Medicine, also provided advice.

Funding was provided by R01 HL054390 from the NHLBI to WAF, the Intramural Research Program of the NIH, NCI, Center for Cancer Research to DDR and MT, and K22 CA128616 to JSI. EPF is a postdoctoral fellow of the American Heart Association.

## References

Bauer, E.M., Qin, Y., Miller, T.W., Bandle, R.W., Csanyi, G., Pagano, P.J., Bauer, P.M., Schnermann, J., Roberts, D.D., and Isenberg, J.S. Thrombospondin-1 supports blood pressure by limiting eNOS activation and endothelial-dependent vasorelaxation. Cardiovasc. Res. Q6

Benton, C.R., Wright, D.C., Bonen, A., 2008. PGC-1alpha-mediated regulation of gene expression and metabolism: implications for nutrition and exercise prescriptions. Appl. Physiol. Nutr. Metab. 33, 843–862.

Booth, F.W., Chakravarthy, M.V., Spangenburg, E.E., 2002. Exercise and gene expression: physiological regulation of the human genome through physical activity. J. Physiol. 543, 399–411.

Bordone, L., Cohen, D., Robinson, A., Motta, M.C., van Veen, E., Czopik, A., Steele, A.D., Crowe, H., Marmor, S., Luo, J., et al., 2007. SIRT1 transgenic mice show phenotypes resembling calorie restriction. Aging Cell 6, 759–767.

Carlezon Jr., W.A., Duman, R.S., Nestler, E.J., 2005. The many faces of CREB. Trends Neurosci. 28, 436–445.

Chang, C.R., Blackstone, C., 2007. Cyclic AMP-dependent protein kinase phosphorylation of Drp1 regulates its GTPase activity and mitochondrial morphology. J. Biol. Chem. 282, 21583–21587.

Chung, J., Wang, X.Q., Lindberg, F.P., Frazier, W.A., 1999. Thrombospondin-1 acts via IAP/CD47 to synergize with collagen in alpha2beta1-mediated platelet activation. Blood 94, 642–648.

Corsetti, G., Pasini, E., D'Antona, G., Nisoli, E., Flati, V., Assanelli, D., Dioguardi, F.S., Bianchi, R., 2008. Morphometric changes induced by amino acid supplementation in skeletal and cardiac muscles of old mice. Am. J. Cardiol. 101, 26E–34E.

Cribbs, J.T., Strack, S., 2007. Reversible phosphorylation of Drp1 by cyclic AMP-dependent protein kinase and calcineurin regulates mitochondrial fission and cell death. EMBO Rep. 8, 939–944.

Duncan, J.G., Fong, J.L., Medeiros, D.M., Finck, B.N., Kelly, D.P., 2007. Insulin-resistant heart exhibits a mitochondrial biogenic response driven by the peroxisome proliferator-activated receptor-alpha/PGC-1alpha gene regulatory pathway. Circulation 115, 909–917.

Feige, J.N., Auwerx, J., 2007. Transcriptional coregulators in the control of energy homeostasis. Trends Cell Biol. 17, 292–301.

Feige, J.N., Auwerx, J., 2008. Transcriptional targets of sirtuins in the coordination of mammalian physiology. Curr. Opin. Cell Biol. 20, 303–309.

Feige, J.N., Lagouge, M., Canto, C., Strehle, A., Houten, S.M., Milne, J.C., Lambert, P.D., Mataki, C., Elliott, P.J., Auwerx, J., 2008. Specific SIRT1 activation mimics low energy levels and protects against diet-induced metabolic disorders by enhancing fat oxidation. Cell Metab. 8, 347–358.

Finck, B.N., Kelly, D.P., 2007. Peroxisome proliferator-activated receptor gamma coactivator-1 (PGC-1) regulatory cascade in cardiac physiology and disease. Circulation 115, 2540–2548.

Frazier, W.A., Gao, A.-G., Dimitry, J., Chung, J., Lindberg, F.P., Brown, E.J., Linder, M.E., 1999. The thrombospondin receptor integrin-associated protein (CD47) functionally couples to heterotrimeric Gi. J. Biol. Chem. 274, 8554–8560.

Guarente, L., 2008. Mitochondria—a nexus for aging, calorie restriction, and sirtuins? Cell 132, 171–176.

Holloszy, J.O., 2008. Regulation by exercise of skeletal muscle content of mitochondria and GLUT4. J. Physiol. Pharmacol. 59 (Suppl. 7), 5–18.

Isenberg, J.S., Calzada, M.J., Zhou, L., Guo, N., Lawler, J., Wang, X.Q., Frazier, W.A., Roberts, D.D., 2005. Endogenous thrombospondin-1 is not necessary for proliferation but is permissive for vascular smooth muscle cell responses to platelet-derived growth factor. Matrix Biol. 24, 110–123.

Isenberg, J.S., Ridnour, L.A., Dimitry, J., Frazier, W.A., Wink, D.A., Roberts, D.D., 2006a. CD47 is necessary for inhibition of nitric oxide-stimulated vascular cell responses by thrombospondin-1. J. Biol. Chem. 281, 26069–26080.

Isenberg, J.S., Wink, D.A., Roberts, D.D., 2006b. Thrombospondin-1 antagonizes nitric oxide-stimulated vascular smooth muscle cell responses. Cardiovasc. Res. 71, 785–793.

Isenberg, J.S., Hyodo, F., Matsumoto, K., Romeo, M.J., Abu-Asab, M., Tsokos, M., Kuppusamy, P., Wink, D.A., Krishna, M.C., Roberts, D.D., 2007a. Thrombospondin-1 limits ischemic tissue survival by inhibiting nitric oxide-mediated vascular smooth muscle relaxation. Blood 109, 1945–1952.

Isenberg, J.S., Hyodo, F., Pappan, L.K., Abu-Asab, M., Tsokos, M., Krishna, M.C., Frazier, W.A., Roberts, D.D., 2007b. Blocking thrombospondin-1/CD47 signaling alleviates deleterious effects of aging on tissue responses to ischemia. Arterioscler. Thromb. Vasc. Biol. 27, 2582–2588.

Isenberg, J.S., Romeo, M.J., Abu-Asab, M., Tsokos, M., Oldenborg, A., Pappan, L., Wink, D.A., Frazier, W.A., Roberts, D.D., 2007c. Increasing survival of ischemic tissue by targeting CD47. Circ. Res. 100, 712–720.

Isenberg, J.S., Frazier, W.A., Krishna, M.C., Wink, D.A., Roberts, D.D., 2008a. Enhancing cardiovascular dynamics by inhibition of thrombospondin-1/CD47 signaling. Curr. Drug Targets 9, 833–841.



Please cite this article as: Frazier, E.P., et al., Age-dependent regulation of skeletal muscle mitochondria by the thrombospondin-1 receptor CD47, Matrix Biology (2011), doi:10.1016/j.matbio.2010.12.004

Isenberg, J.S., Frazier, W.A., Roberts, D.D., 2008b. Thrombospondins: from structure to therapeutics: thrombospondin-1: a physiological regulator of nitric oxide signaling. Cell. Mol. Life Sci. 65, 728–742.

Isenberg, J.S., Maxhimer, J.B., Hyodo, F., Pendrak, M.L., Ridnour, L.A., DeGraff, W.G., Tsokos, M., Wink, D.A., Roberts, D.D., 2008c. Thrombospondin-1 and CD47 limit cell and tissue survival of radiation injury. Am. J. Pathol. 173, 1100–1112.

Isenberg, J.S., Maxhimer, J.B., Powers, P., Tsokos, M., Frazier, W.A., Roberts, D.D., 2008d. Treatment of liver ischemia-reperfusion injury by limiting thrombospondin-1/CD47 signaling. Surgery 144, 752–761.

Isenberg, J.S., Pappan, L.K., Romeo, M.J., Abu-Asab, M., Tsokos, M., Wink, D.A., Frazier, W. A., Roberts, D.D., 2008e. Blockade of thrombospondin-1-CD47 interactions prevents necrosis of full thickness skin grafts. Ann. Surg. 247, 180–190.

Isenberg, J.S., Roberts, D.D., Frazier, W.A., 2008f. CD47: a new target in cardiovascular therapy. Arterioscler. Thromb. Vasc. Biol. 28, 615–621.

Isenberg, J.S., Romeo, M.J., Yu, C., Yu, C.K., Nghiem, K., Monsale, J., Rick, M.E., Wink, D.A., Frazier, W.A., Roberts, D.D., 2008g. Thrombospondin-1 stimulates platelet aggregation by blocking the antithrombotic activity of nitric oxide/cGMP signaling. Blood 111, 613–623.

Isenberg, J.S., Qin, Y., Maxhimer, J.B., Sipes, J.M., Despres, D., Schnermann, J., Frazier, W. A., Roberts, D.D., 2009. Thrombospondin-1 and CD47 regulate blood pressure and cardiac responses to vasoactive stress. Matrix Biol. 28, 110–119.

Jin, G., Tsuji, K., Xing, C., Yang, Y.G., Wang, X., Lo, E.H., 2009. CD47 gene knockout protects against transient focal cerebral ischemia in mice. Exp. Neurol. 217, 165–170.

Katic, M., Kennedy, A.R., Leykin, I., Norris, A., McGettrick, A., Gesta, S., Russell, S.J., Bluher, M., Maratos-Flier, E., Kahn, C.R., 2007. Mitochondrial gene expression and increased oxidative metabolism: role in increased lifespan of fat-specific insulin receptor knock-out mice. Aging Cell 6, 827–839.

Lagouge, M., Argmann, C., Gerhart-Hines, Z., Meziane, H., Lerin, C., Daussin, F., Messadeq, N., Milne, J., Lambert, P., Elliott, P., et al., 2006. Resveratrol improves mitochondrial function and protects against metabolic disease by activating SIRT1 and PGC-1alpha. Cell 127, 1109–1122.

Lai, L., Leone, T.C., Zechner, C., Schaeffer, P.J., Kelly, S.M., Flanagan, D.P., Medeiros, D.M., Kovacs, A., Kelly, D.P., 2008. Transcriptional coactivators PGC-1alpha and PGC-lbeta control overlapping programs required for perinatal maturation of the heart. Genes Dev. 22, 1948–1961.

Le Gouill, E., Jimenez, M., Binnert, C., Jayet, P.Y., Thalmann, S., Nicod, P., Scherrer, U., Vollenweider, P., 2007. Endothelial nitric oxide synthase (eNOS) knockout mice have defective mitochondrial beta-oxidation. Diabetes 56, 2690–2696.

Leone, T.C., Lehman, J.J., Finck, B.N., Schaeffer, P.J., Wende, A.R., Boudina, S., Courtois, M., Wozniak, D.F., Sambandam, N., Bernal-Mizrachi, C., et al., 2005. PGC-1alpha deficiency causes multi-system energy metabolic derangements: muscle dysfunction, abnormal weight control and hepatic steatosis. PLoS Biol. 3, e101.

Lin, J., Wu, H., Tarr, P.T., Zhang, C.Y., Wu, Z., Boss, O., Michael, L.F., Puigserver, P., Isotani, E., Olson, E.N., et al., 2002. Transcriptional co-activator PGC-1 alpha drives the formation of slow-twitch muscle fibres. Nature 418, 797–801.

Lin, J., Handschin, C., Spiegelman, B.M., 2005. Metabolic control through the PGC-1 family of transcription coactivators. Cell Metab. 1, 361–370.

Lindberg, F.P., Bullard, D.C., Caver, T.E., Gresham, H.D., Beaudet, A.L., Brown, E.J., 1996. Decreased resistance to bacterial infection and granulocyte defects in IAP-deficient mice. Science 274, 795–798.

Lira, V.A., Benton, C.R., Yan, Z., and Bonen, A. PGC-1alpha regulation by exercise training and its influences on muscle function and insulin sensitivity. Am. J. Physiol. Endocrinol. Metab. 299, E145-161.

Lira, V.A., Brown, D.L., Lira, A.K., Kavazis, A.N., Soltow, Q.A., Zeanah, E.H., and Criswell, D. S. Nitric oxide and AMPK cooperatively regulate PGC-1 in skeletal muscle cells. J. Physiol. 588, 3551-3566.

Lopez-Lluch, G., Hunt, N., Jones, B., Zhu, M., Jamieson, H., Hilmer, S., Cascajo, M.V., Allard, J., Ingram, D.K., Navas, P., et al., 2006. Calorie restriction induces mitochondrial biogenesis and bioenergetic efficiency. Proc. Natl Acad. Sci. USA 103, 1768–1773.

Malek, M.H., Olfert, I.M., 2009. Global deletion of thrombospondin-1 increases cardiac and skeletal muscle capillarity and exercise capacity in mice. Exp. Physiol. 94, 749–760.

Manna, P.P., Frazier, W.A., 2003. The mechanism of CD47-dependent killing of T cells: heterotrimeric Gi-dependent inhibition of protein kinase A. J. Immunol. 170, 3544–3553.

Maxhimer, J.B., Shih, H.B., Isenberg, J.S., Miller, T.W., Roberts, D.D., 2009. Thrombospondin-1/CD47 blockade following ischemia–reperfusion injury is tissue protective. Plast. Reconstr. Surg. 124, 1880–1889.

Miller, T.W., Isenberg, J.S., and Roberts, D.D. Thrombospondin-1 is an inhibitor of pharmacological activation of soluble guanylate cyclase. Br. J. Pharmacol. 159, 1542-1547.

Nemoto, S., Fergusson, M.M., Finkel, T., 2005. SIRT1 functionally interacts with the metabolic regulator and transcriptional coactivator PGC-1{alpha}. J. Biol. Chem. 280, 16456–16460.

Nisoli, E., Carruba, M.O., 2006. Nitric oxide and mitochondrial biogenesis. J. Cell Sci. 119, 2855–2862.

Nisoli, E., Falcone, S., Tonello, C., Cozzi, V., Palomba, L., Fiorani, M., Pisconti, A., Brunelli, S., Cardile, A., Francolini, M., et al., 2004. Mitochondrial biogenesis by NO yields functionally active mitochondria in mammals. Proc. Natl Acad. Sci. USA 101, 16507–16512.

Oh, M., Rybkin, I.I., Copeland, V., Czubryt, M.P., Shelton, J.M., van Rooij, E., Richardson, J. A., Hill, J.A., De Windt, L.J., Bassel-Duby, R., et al., 2005. Calcineurin is necessary for the maintenance but not embryonic development of slow muscle fibers. Mol. Cell. Biol. 25, 6629–6638.

Rodgers, J.T., Lerin, C., Haas, W., Gygi, S.P., Spiegelman, B.M., Puigserver, P., 2005. Nutrient control of glucose homeostasis through a complex of PGC-1alpha and SIRT1. Nature 434, 113–118.

Salminen, A., Kaarniranta, K., 2009. SIRT1: regulation of longevity via autophagy. Cell. Signal. 21, 1356–1360.

Scherz-Shouval, R., Elazar, Z., 2007. ROS, mitochondria and the regulation of autophagy. Trends Cell Biol. 17, 422–427.

Scherz-Shouval, R., Shvets, E., Fass, E., Shorer, H., Gil, L., Elazar, Z., 2007. Reactive oxygen species are essential for autophagy and specifically regulate the activity of Atg4. EMBO J. 26, 1749–1760.

Schmidt, R.E., Green, K.G., Snipes, L.L., Feng, D., 2009. Neuritic dystrophy and neuronopathy in Akita (Ins2(Akita)) diabetic mouse sympathetic ganglia. Exp. Neurol. 216, 207–218.

Shiva, S., Sack, M.N., Greer, J.J., Duranski, M., Ringwood, L.A., Burwell, L., Wang, X., MacArthur, P.H., Shoja, A., Raghavachari, N., et al., 2007. Nitrite augments tolerance to ischemia/reperfusion injury via the modulation of mitochondrial electron transfer. J. Exp. Med. 204, 2089–2102.

Spangenburg, E.E., Booth, F.W., 2003. Molecular regulation of individual skeletal muscle fibre types. Acta Physiol. Scand. 178, 413–424.

Timmers, H.J., Pacak, K., Huynh, T.T., Abu-Asab, M., Tsokos, M., Merino, M.J., Baysal, B.E., Adams, K.T., Eisenhofer, G., 2008. Biochemically silent abdominal paragangliomas in patients with mutations in the succinate dehydrogenase subunit B gene. J. Clin. Endocrinol. Metab. 93, 4826–4832.

Uldry, M., Yang, W., St-Pierre, J., Lin, J., Seale, P., Spiegelman, B.M., 2006. Complementary action of the PGC-1 coactivators in mitochondrial biogenesis and brown fat differentiation. Cell Metab. 3, 333–341.

Uluckan, O., Becker, S.N., Deng, H., Zou, W., Prior, J.L., Piwnica-Worms, D., Frazier, W.A., Weilbaecher, K.N., 2009. CD47 regulates bone mass and tumor metastasis to bone. Cancer Res. 69, 3196–3204.

Wang, X.Q., Lindberg, F.P., Frazier, W.A., 1999. Integrin-associated protein stimulates alpha2beta1-dependent chemotaxis via Gi-mediated inhibition of adenylate cyclase and extracellular-regulated kinases. J. Cell Biol. 147, 389–400.

Wenz, T., Rossi, S.G., Rotundo, R.L., Spiegelman, B.M., Moraes, C.T., 2009. Increased muscle PGC-1alpha expression protects from sarcopenia and metabolic disease during aging. Proc. Natl Acad. Sci. USA 106, 20405–20410.

Wozniak, A.C., Anderson, J.E., 2007. Nitric oxide-dependence of satellite stem cell activation and quiescence on normal skeletal muscle fibers. Dev. Dyn. 236, 240–250.

Wu, Z., Huang, X., Feng, Y., Handschin, C., Feng, Y., Gullicksen, P.S., Bare, O., Labow, M., Spiegelman, B., Stevenson, S.C., 2006. Transducer of regulated CREB-binding proteins (TORCs) induce PGC-1alpha transcription and mitochondrial biogenesis in muscle cells. Proc. Natl Acad. Sci. USA 103, 14379–14384.

Yao, M., Roberts, D.D., and Isenberg, J.S., in press. Thrombospondin-1 inhibition of vascular smooth muscle cell responses occurs via modulation of both cAMP and cGMP. Pharmacol Res.




Please cite this article as: Frazier, E.P., et al., Age-dependent regulation of skeletal muscle mitochondria by the thrombospondin-1 receptor CD47, Matrix Biology (2011), doi:10.1016/j.matbio.2010.12.004